

JURNAL

by Jurnal_pa Nurhadi Buat Pak Gb_2

Submission date: 23-Jan-2019 03:04PM (UTC+0700)

Submission ID: 1067425973

File name: Modification_of_Coal_Char-loaded_TiO2_by_Sulfonation.pdf (603.18K)

Word count: 4075

Character count: 20106



Research Article

Modification of Coal Char-loaded TiO₂ by Sulfonation and Alkylsilylation to Enhance Catalytic Activity in Styrene Oxidation with Hydrogen Peroxide as Oxidant

Mukhamad Nurhadi

Department of Chemical Education, Universitas Mulawarman,
Kampus Gunung Kelua, Samarinda, 75119, East Kalimantan, Indonesia

Received: 24th May 2016; Revised: 11st October 2016; Accepted: 18th October 2016

Abstract

The modified coal char from low-rank coal by sulfonation, titanium impregnation and followed by alkyl silylation possesses high catalytic activity in styrene oxidation. The surface of coal char was undergone several steps as such: modification using concentrated sulfuric acid in the sulfonation process, impregnation of 500 mmol titanium(IV) isopropoxide and followed by alkyl silylation of n-octadecyltrichlorosilane (OTS). The catalysts were characterized by X-ray diffraction (XRD), IR spectroscopy, nitrogen adsorption, and hydrophobicity. The catalytic activity of the catalysts has been examined in the liquid phase styrene oxidation by using aqueous hydrogen peroxide as oxidant. The catalytic study showed the alkyl silylation could enhance the catalytic activity of Ti-SO₃H/CC-600(2.0). High catalytic activity and reusability of the o-Ti-SO₃H/CC-600(2.0) were related to the modification of local environment of titanium active sites and the enhancement the hydrophobicity of catalyst particle by alkyl silylation. Copyright © 2017 BCREC GROUP. All rights reserved

Keywords: styrene; oxidation; coal char; sulfonation; alkylsilylation

How to Cite: Nurhadi, M. (2017). Modification of Coal Char-loaded TiO₂ by Sulfonation and Alkylsilylation to Enhance Catalytic Activity in Styrene Oxidation with Hydrogen Peroxide as Oxidant. *Bulletin of Chemical Reaction Engineering & Catalysis*, 12 (1): 55-61 (doi:10.9767/bcrec.12.1.501.55-61)

Permalink/DOI: <http://dx.doi.org/10.9767/bcrec.12.1.501.55-61>

1. Introduction

Coal is very cheap, readily obtainable and most abundant in Indonesia. Coal resources in this country have been predicted about 21.13 billion short tons and it was dominated by low rank coal which consists of lignite and sub-bituminous. Thus, Indonesia has become the second largest coal supplier in the world [1]. Pyrolysis and gasification process of coal produce coal char as the by-product. Recently, it has been found a new class and cheap catalyst support with superior performance. Many re-

searches have been reported about the usage of coal char as catalyst support such as coal char supported iron and coal char supported nickel for tar reforming process [2]. Superior performance from coal char as catalyst support can be created by sulfonation and alkylsilylation process.

Sulfonation with concentrated sulfuric acid is aimed to form the hydrophilic functional group, such as -SO₃H, -COOH and phenolic -OH group on coal char surface. Hydrophilic functional group on coal char surface leads to good access TiO₂ to be incorporated on the coal char surface as a catalyst, which gives rise to high catalytic performance, despite the low sur-

* Corresponding Author.
E-mail: nurhadi1969@yahoo.co.id

face area [3]. Sulfonation of such as coal char materials is thus expected to provide a highly stable solid with a high density of active sites, allowing high performance of catalysts [4]. In order to increase the stability of mesoporous material, alkyl silylation is employed to produce highly hydrophobic materials, and to increase the catalytic activity of Ti modified catalyst in epoxidation alkenes using H₂O₂ as oxidant agent [5]. The alkylsilyl groups served as a template to prevent irreversible adsorption of reactant and keep the active site free from the self poisoning [6].

Prompted by this several factors of improving coal char as a catalyst, we have examined surface modification of coal char by sulfonation, impregnation TiO₂ and continued with functionalization of silane coupling agent. We found that surface alkyl silylation of sulfonated coal char that impregnated TiO₂ exert a promoting effect in the oxidation of styrene.

2. Materials and Method

2.1. Raw materials

The parent coal from Batuah, Loa jannan, Kutai Kartanegara East Kalimantan, Indonesia has been used as raw material. Based on previous research, the coal ranking was determined as low rank coal from the proximate and ultimate analysis [7].

2.2. Catalyst preparation

The coal (200 mesh) was pyrolyzed in a fluidized bed unit under the nitrogen atmosphere by using gas flow rate 100 cc/min, at 600 °C for 2 h, and by heating rate 5 °C/min. The coal char obtained in this pyrolysis was labeled as CC-600(2.0).

The sulfonation process to the CC-600(2.0) was carried out by adding 12 mL of 98 % sulfuric acid (JT Beker) per gram of coal. The mixture was stirred and heated in an oil bath at 90 °C for 12 h. The solid product was washed with warm distilled water at 80 °C to remove sulfate ions, and it was dried at 110 °C for overnight. Coal char which was sulfonated indicating as sulfonated coal char (SO₃H/CC-600(2.0)). Furthermore, titanium tetra-isopropoxide (97 %, Aldrich) which contained the molar amount of

titanium(IV) ion (500 μmol g⁻¹) in toluene was impregnated into SO₃H/CC-600(2.0) by vigorous stirring at room temperature until toluene completely evaporated. Subsequently, the solid was washed with ethanol to remove toluene and dried at 110 °C. The catalyst that obtained was signed Ti-SO₃H/CC-600(2.0).

For the alkylsilylation process, 95% n-octadecyltrichlorosilane (OTS, CH₃(CH₂)₁₇SiCl₃, Merck) was used. The 1 g of Ti-(SO₃H/CC-600(2.0) catalyst was mixed in 10 ml of toluene solution containing 500 μmol of OTS, shaking for 5 minutes at room temperature. The mixture was centrifuged to remove unreacted OTS and washed with ethanol for 3 times. The solid catalyst was dried at 110 °C for overnight. The catalyst was labeled as o-Ti-(SO₃H/CC-600(2.0)). A complete list of the codes and treatments used in this research can be seen in Table 1.

2.3. Samples characterization

All catalysts were characterized by using the Infrared (IR), X-ray diffraction (XRD), Nitrogen adsorption-desorption, Scanning electron microscopy (SEM) and Hydrophobicity. IR spectra of the catalysts were recorded on a Perkin Elmer Fourier transform infrared (FTIR) spectrometer, with a spectral resolution of 2 cm⁻¹, scans 10 s, at temperature 20 °C. The XRD patterns were collected with a Bruker AXS Advance D8 diffractometer using Cu K_α radiation (λ = 1.5405 Å, 40 kV and 40 mA). The surface area of the catalysts was determined by using a Micromeritics ASAP 2020 V4.00 surface area analyzer by nitrogen adsorption at 77 K. The pore size distribution was evaluated using the Barrett-Joyner-Halenda (BJH) model. Scanning electron microscopy, photographs, and elemental analysis in the solid particles were obtained by using JEOL JSM-6390LV instrument with an accelerating voltage of 15 kV. The hydrophobicity was calculated based on the amount adsorbed water in the catalysts. Determination of hydrophobicity followed procedure described by Nurhadi *et al.* [8].

2.4. Catalytic test

The catalytic tests were carried out by oxidizing styrene using 30% aqueous H₂O₂ as oxi-

Table 1. Codes and treatments done to the samples

| Samples | Type of treatment | Time of sulfonation (h) | Temperature of pyrolysis | Time of pyrolysis (h) |
|-------------------------------------|-------------------|-------------------------|--------------------------|-----------------------|
| Ti-SO ₃ H/CC-600 (2.0) | Sulfonation | 12 | 600 | 2.0 |
| o-Ti-SO ₃ H/CC-600 (2.0) | Sulfonation | 12 | 600 | 2.0 |

dant. The catalytic tests were carried out according to the modification procedure reported previously [9]. All reactions were carried out at room temperature for 20 h under stirring with styrene (5 mmol), 30 % aqueous H₂O₂ (5 mmol), acetonitrile (4.5 ml), and catalyst (50 mg). The products of the reaction were analyzed by GC-2014 Shimadzu-gas chromatograph.

3. Results and Discussion

3.1. Physical properties

Figure 1 shows the XRD pattern of coal char, Ti-SO₃H/CC-600(2.0) and o-Ti-SO₃H/CC-600(2.0). Based on JSPDF number 00-026-1079, both of the catalysts show peaks at $2\theta = 26.6^\circ$, 43.5° , and 46.3° which are assigned to turbostratic graphite structure. All patterns also possess the crystalline structure at 26.5° which is attributed to quartz [10,11]. The XRD pattern of o-Ti-SO₃H/CC-600(2.0) exhibits different broad peak at 2θ range 10° - 20° which is assigned to amorphous silica that attaches on the surface of Ti-SO₃H/CC-600(2.0) catalyst after alkyl silylation process.

The FTIR spectra for Ti-SO₃H/CC-600(2.0) and o-Ti-SO₃H/CC-600(2.0) are shown in Figure 2. The FTIR spectra of both samples show a broad band at around 3416 cm^{-1} which were attributed to the O-H stretching mode of the -COOH and phenolic OH groups [12]. The intensity of OH groups increased after the long carbon chains of alkylsilyl groups attached on Ti-SO₃H/CC-600(2.0) surface. From the appear-

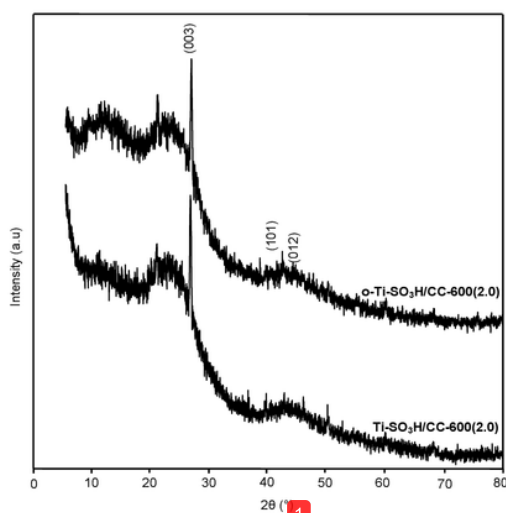


Figure 1. XRD pattern of Ti-SO₃H/CC-600(2.0) and o-Ti-SO₃H/CC-600(2.0)

ance of peaks at around 2912 and 2844 cm^{-1} shown in Figure 2 (o-Ti-SO₃H/CC-600(2.0)) that assigned to symmetric and asymmetric stretching mode of the C-H sp³ groups and correlated the peak at 1462 cm^{-1} was attributed as bending mode of C-H as the evident the long carbon chains of alkylsilyl groups have attached on the Ti-SO₃H/CC-600(2.0) surface [13]. The peak at around 1619 cm^{-1} correlated to bending mode of the aromatic-like C=C stretching mode in polyaromatics and graphite-like materials. The peak at around 1088 cm^{-1} was attributed to the asymmetric stretching of Si-O-Si groups. The symmetric stretching modes of Si-O-Si groups are investigated at around 789 cm^{-1} . The peak intensity that shows the existence framework silica at around 1088 and 789 cm^{-1} (Figure 2 (o-Ti-SO₃H/CC-600(2.0))) increase and this an evident that the silica from OTS has attached on Ti-SO₃H/CC-600(2.0) surface. The weak peak at around 1034 cm^{-1} shown in Figure 2 (Ti-SO₃H/CC-600(2.0)) and the peak at around 571 cm^{-1} are assigned the presence S=O symmetric stretching mode and the SO₂ deformation frequency that indicate the presence -SO₃H groups attachment on the surface [14]. The existence of framework titanium was characterized by an adsorption band in the 900 - 975 cm^{-1} but both spectra as shown in Figure 2 were not detected and only a peak at around 462 cm^{-1} was attributed to the symmetric O-Ti-O stretching that caused the vibration of Ti-O bond.

The effects of the presence of n-octadecyltrichlorosilane (OTS) on the surface area and porous structure of Ti-SO₃H/CC-600(2.0) were determined by the analysis of Nitrogen adsorption-desorption isotherms. Figure

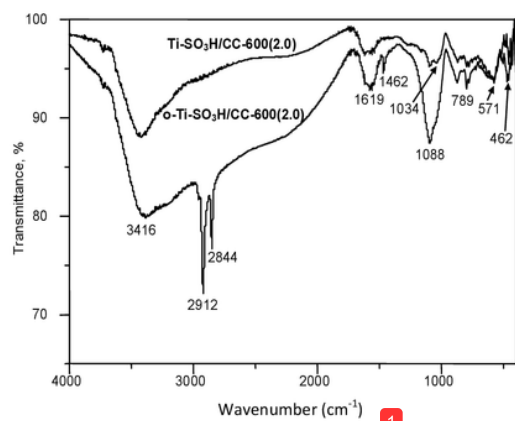


Figure 2. FTIR spectra of Ti-SO₃H/CC-600(2.0) and o-Ti-SO₃H/CC-600(2.0).

3 shows nitrogen adsorption-desorption isotherms and pore size distributions of $\text{Ti-SO}_3\text{H/CC-600(2.0)}$ and $o\text{-Ti-SO}_3\text{H/CC-600(2.0)}$. Both isotherms were of Type IV in the IUPAC classifications, which are a typical isotherm for mesoporous materials. The isotherms exhibited that clear hysteresis loops in the relative pressure range $\sim 0.14\text{-}1.0$ ($\text{Ti-SO}_3\text{H/CC-600(2.0)}$) and $\sim 0.45\text{-}0.99$ ($o\text{-Ti-SO}_3\text{H/CC-600(2.0)}$). The pore size distribution indicates the presence of uniform mesopores ~ 79 Å ($\text{Ti-SO}_3\text{H/CC-600(2.0)}$) and ~ 135 Å ($o\text{-Ti-SO}_3\text{H/CC-600(2.0)}$). After $\text{Ti-SO}_3\text{H/CC-600(2.0)}$ was modified with OTS, the BET surface area, total pore volume and mean pore sizes of $o\text{-Ti-SO}_3\text{H/CC-600(2.0)}$ decrease as shown in Table 2. This decrease was due to the OTS that probably coated the $\text{Ti-SO}_3\text{H/CC-600(2.0)}$ surface in the form of a monolayer. The molecular length of OTS around 2.6 nm [15,16] meanwhile the average pore of $\text{Ti-SO}_3\text{H/CC-600(2.0)}$ is 19.7 nm, where it would be easy for OTS to react with the external and internal pore surfaces. The result shows that $o\text{-Ti-SO}_3\text{H/CC-600(2.0)}$ possesses hydrophobic external and internal surfaces. The long carbon chains from OTS that dispersed on $\text{Ti-SO}_3\text{H/CC-600(2.0)}$ surface lead to a decrease in the BET surface area, total pore volume and mean pore sizes. It is because the

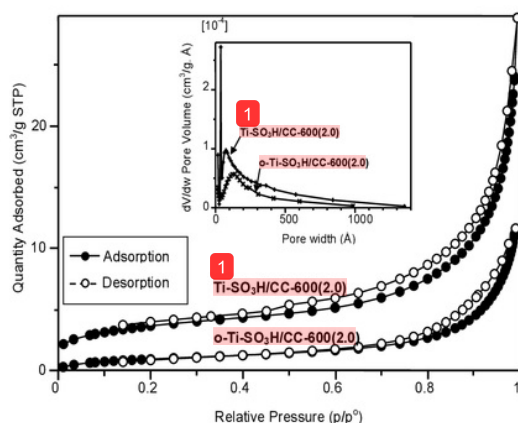


Figure 3. N_2 adsorption-desorption isotherms and BJH pore distribution of $\text{Ti-SO}_3\text{H/CC-600(2.0)}$ and $o\text{-Ti-SO}_3\text{H/CC-600(2.0)}$

size of OTS less than the average pore size of $\text{Ti-SO}_3\text{H/CC-600(2.0)}$, OTS probably will block the pore of $\text{Ti-SO}_3\text{H/CC-600(2.0)}$ which size is smaller than 2.6 nm and OTS also will fill in the larger pores of $\text{Ti-SO}_3\text{H/CC-600(2.0)}$, the average pore volume of $o\text{-Ti-SO}_3\text{H/CC-600(2.0)}$ smaller than that of $\text{Ti-SO}_3\text{H/CC-600(2.0)}$.

Figure 4 shows SEM images of $\text{Ti-SO}_3\text{H/CC-600(2.0)}$ and $o\text{-Ti-SO}_3\text{H/CC-600(2.0)}$. Both of the samples reveal different surface morphologies. The small agglomerations of titanium appear on $\text{Ti-SO}_3\text{H/CC-600(2.0)}$ surface, and it becomes big after underwent alkyl silylation.

Figure 5 shows the percentage of adsorbed water of $\text{Ti-SO}_3\text{H/CC-600(2.0)}$ and $o\text{-Ti-SO}_3\text{H/CC-600(2.0)}$. The percentage of adsorbed water of $\text{Ti-SO}_3\text{H/CC-600(2.0)}$ was significantly higher than $o\text{-Ti-SO}_3\text{H/CC-600(2.0)}$. Apparently, the titanium impregnation leads to the changes in oxygen functional groups as titanyl

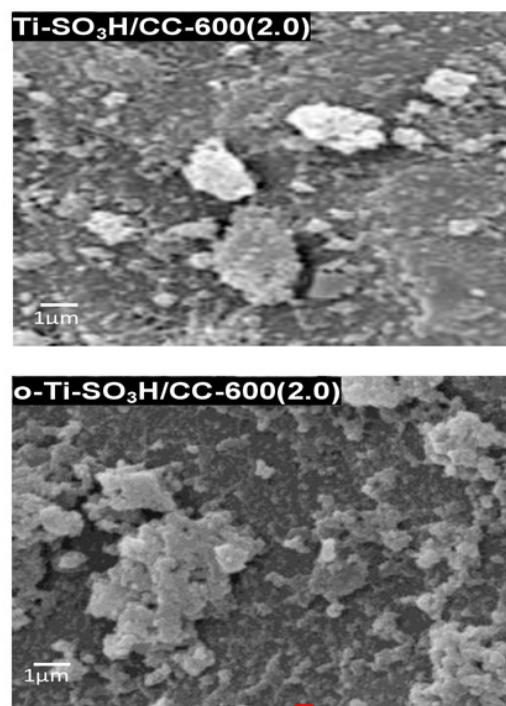


Figure 4. SEM images of $\text{Ti-SO}_3\text{H/CC-600(2.0)}$ and $o\text{-Ti-SO}_3\text{H/CC-600(2.0)}$

Table 2. Physical properties of catalysts

| Samples | BET surface area | Pore Volume (cm^3/g) | Mean pore size | Average hydrophobicity (%wt) |
|--|------------------|--|----------------|------------------------------|
| $\text{Ti-SO}_3\text{H/CC-600(2.0)}$ | 12.86 | 0.042 | 19.71 | 5.22 |
| $o\text{-Ti-SO}_3\text{H/CC-600(2.0)}$ | 3.59 | 0.018 | 17.80 | 5.09 |

(Ti=O) and titanol (Ti–OH) groups on $\text{SO}_3\text{H}/\text{CC-600}(2.0)$ surface, that it increases the interaction with H_2O . Alkyl silylation to $\text{Ti-SO}_3\text{H}/\text{CC-600}(2.0)$ causes alkylsilyl groups should be attached and covered with the external and internal surfaces of $\text{Ti-SO}_3\text{H}/\text{CC-600}(2.0)$ that it can prevent and decrease the interaction with H_2O .

3.2. Catalytic activity

Figure 6 shows a histogram of yields of products from styrene oxidation catalyzed by $\text{Ti-SO}_3\text{H}/\text{CC-600}(2.0)$ and $o\text{-Ti-SO}_3\text{H}/\text{CC-600}(2.0)$. The product yields of styrene oxidation using H_2O_2 as an oxidant were benzaldehyde, phenyl acetaldehyde, and styrene oxide. It is observed that the yield of benzaldehyde was 0.558 mmol at room temperature for 20 h with $\text{Ti-SO}_3\text{H}/\text{CC-600}(2.0)$ catalyst, and the yield decreased when $o\text{-Ti-SO}_3\text{H}/\text{CC-600}(2.0)$ was used as the catalyst, indicating that $\text{Ti-SO}_3\text{H}/\text{CC-600}(2.0)$ has lower catalytic activities in this reaction. The yield of phenyl acetal-

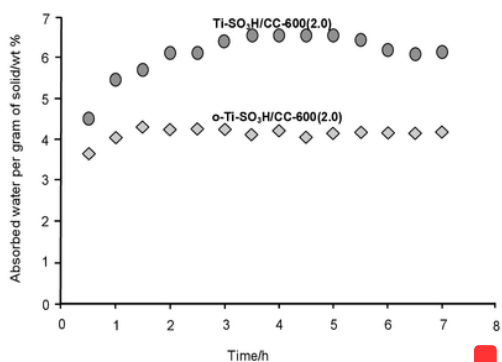


Figure 5. Water adsorption percentage for $\text{Ti-SO}_3\text{H}/\text{CC-600}(2.0)$, and $o\text{-Ti-SO}_3\text{H}/\text{CC-600}(2.0)$

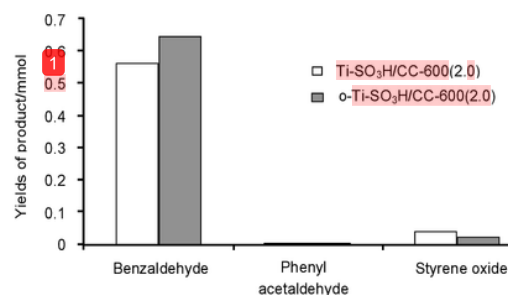


Figure 6. Comparison of catalytic activity of $\text{Ti-SO}_3\text{H}/\text{CC600}(2.0)$ and $o\text{-Ti-SO}_3\text{H}/\text{CC600}(2.0)$ in the oxidation of styrene (5 mmol), 30% H_2O_2 (5 mmol) and catalyst (50 mg). The yield of product at room temperature for 20 h

dehyde from both catalysts almost undetected due to the amount of the product was terribly small. The yield of styrene oxide of $\text{Ti-SO}_3\text{H}/\text{CC-600}(2.0)$ was two-fold increase when $o\text{-Ti-SO}_3\text{H}/\text{CC-600}(2.0)$ was used as a catalyst.

The high yield of benzaldehyde has led it to act as a dominant product in styrene oxidation after alkyl silylation can be explained on the basis of an increase in the hydrophobicity of $o\text{-Ti-SO}_3\text{H}/\text{CC-600}(2.0)$ catalyst. When the styrene and H_2O_2 as the substrates make interaction with titanium(IV) as the active sites, H_2O_2 releases H_2O as the side product. The hydrophobic long carbon chains of alkylsilyl groups can prevent the H_2O from interacting with titanium(IV) active sites, hence it has not been poisoned and deactivated by H_2O , and consequently the catalytic activity has increased.

In order to investigate the capability to be reused and stability of the $\text{Ti-SO}_3\text{H}/\text{CC-600}(2.0)$ and $o\text{-Ti-SO}_3\text{H}/\text{CC-600}(2.0)$, both catalysts were recovered and recycled for further reaction. After each use, both catalysts were recycled by washing with ethanol and centrifugation thrice and drying at 110 °C in a vacuum oven for overnight. The yield of benzaldehyde was used as basis to compare both catalysts. As shown in Figure 7, it can be seen that the $o\text{-Ti-SO}_3\text{H}/\text{CC-600}(2.0)$ catalyst, the activity was higher and more stable after three reaction cycles than $\text{Ti-SO}_3\text{H}/\text{CC-600}(2.0)$ catalyst and the decrease of the yield of benzaldehyde from the first reaction cycle to second and third reaction cycle was 0.643 mmol to 0.520 mmol and 0.63 mmol, accordingly. Different from the $o\text{-Ti-SO}_3\text{H}/\text{CC-600}(2.0)$ catalyst, $\text{Ti-SO}_3\text{H}/\text{CC-600}(2.0)$ catalyst showed the yield of benzaldehyde was drastically decreased from 0.558 mmol to 0.223 mmol and 0.132 mmol, accor-

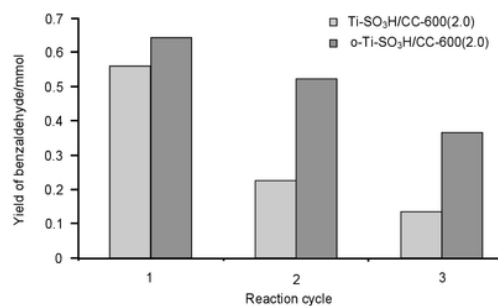


Figure 7. The capability to be reused of $\text{Ti-SO}_3\text{H}/\text{CC600}(2.0)$ and $o\text{-Ti-SO}_3\text{H}/\text{CC600}(2.0)$ in the oxidation of styrene (5 mmol), 30% H_2O_2 (5 mmol) and catalyst (50 mg). The yield of benzaldehyde at room temperature for 20 h

dingly. Based on catalytic activity for styrene oxidation with H_2O_2 as oxidant, after three cycles of reaction and wash, it is predicted that around 50% of the $o\text{-Ti-SO}_3\text{H/CC-600(2.0)}$ and 20% of $\text{Ti-SO}_3\text{H/CC-600(2.0)}$ catalytic sites of freshly catalysts should remain on the catalyst under the reaction conditions used in this study. The explanation that might be used is the physical loss of some catalyst powder during the recycle process. During the washing step of $o\text{-Ti-SO}_3\text{H/CC-600(2.0)}$, the presence of alkylsilyl groups that covered titanium(IV) active sites, it can prevent the leaching and dissolving of titanium(IV) active sites into ethanol solvent. On the contrary, for $\text{Ti-SO}_3\text{H/CC-600(2.0)}$, the leaching was unavoidable because titanium(IV) active sites have direct interaction with the ethanol solvent during the washing steps.

4. Conclusions

The results explained above describe that $\text{Ti-SO}_3\text{H/CC-600(2.0)}$ and $o\text{-Ti-SO}_3\text{H/CC-600(2.0)}$ were successfully created, their properties exist due to the presence of titanium(IV) active sites on their surface. Various characterizations of $\text{Ti-SO}_3\text{H/CC-600(2.0)}$ and $o\text{-Ti-SO}_3\text{H/CC-600(2.0)}$ samples showed that, both samples were amorphous, mesoporous, and attachment of the long carbon chain of alkylsilyl groups on $\text{Ti-SO}_3\text{H/CC-600(2.0)}$ surface can increase the hydrophobicity. The catalytic performance of $o\text{-Ti-SO}_3\text{H/CC-600(2.0)}$ showed the increase due to effect of alkyl silylation process of $\text{Ti-SO}_3\text{H/CC-600(2.0)}$. The catalytic activity in styrene oxidation with aqueous hydrogen peroxide as an oxidant of $o\text{-Ti-SO}_3\text{H/CC-600(2.0)}$ was higher than $\text{Ti-SO}_3\text{H/CC-600(2.0)}$. The increment of catalytic activity of $o\text{-Ti-SO}_3\text{H/CC-600(2.0)}$ can be considered as the influence of its hydrophobicity.

Acknowledgements

The author is grateful to the funding from government East Kalimantan, Indonesia.

References

- Hasan, M.H., Mahlia, T.M.I., Nur, H. (2012). A Review on Energy Scenario and Sustainable Energy in Indonesia. *Renew. Sust. Energ. Rev.* 16(4): 2316-2328.
- Min, Z., Asadullah, M., Yimsiri, P., Zhang, S., Wu, H., Li, C.Z. (2011). Catalytic Reforming of Tar during Gasification. Part I. Steam Reforming of Biomass Tar using Ilmenite as a Catalyst. *Fuel.* 90(5): 1847-1854.
- Suganuma, S., Nakajima, K., Kitano, M., Yamaguchi, D., Kato, H. (2010). Synthesis and Acid Catalysis of Cellulose-derived Carbon-based Solid Acid. *Solid State Sci.* 12(12): 1029-1034.
- Takagaki, A., Toda, M., Okamura, M., Kondo, J.N., Hayashi, S., Domen, K., Hara, M. (2006). Esterification of Higher Fatty Acids by a Novel Strong Solid Acid. *Catal. Today.* 116(2): 157-161.
- Badiei, A., Bonneviot, L., Crowther, N., Mohammadi Ziarani, G. (2006). Surface Tailoring Control in Micelle Templated Silica. *J. Organomet. Chem.* 691(26): 5911-5919.
- Imizu, Y., Narita, T., Fujito, Y., Yamada, H. (2000). Zinc Oxide Modified by Alkylsilylation as an Efficient Catalyst for Isomerization of Hydrocarbon. In F.V.M.S.M. Avelino Corma and G.F. José Luis (Eds.), *Stud. Surf. Sci. Catal.* 130: 2429-2434.
- Nurhadi, M., Efendi, J., Ling, L.S., Mahlia, T.M.I., Siang, H.C., Yuan, L.S., Nur, H. (2014). Titanium Dioxide-Supported Sulfonated Low Rank Coal as Catalysts in the Oxidation of Styrene with Aqueous Hydrogen Peroxide. *J. Teknologi.* 69(5): 71-79
- Nurhadi, M., Efendi, J., Lee, S.L., Mahlia, T. M.I., Chandren, S., Ho, C.S., Nur, H. (2015). Utilization of Low Rank Coal as Oxidation Catalyst by Controllable Removal of its Carbonaceous Component. *J. Taiwan Inst. Chem. Eng.* 46(0): 183-190.
- Zhan, W., Guo, Y., Wang, Y., Guo, Y., Liu, X., Wang, Y., Lu, G. (2009). Study of Higher Selectivity to Styrene Oxide in the Epoxidation of Styrene with Hydrogen Peroxide over La-Doped MCM-48 Catalyst. *J. Phys. Chem. C.* 113(17): 7181-7185.
- Liu, Y., Chen, J., Yao, J., Lu, Y., Zhang, L., Liu, X. (2009). Preparation and Properties of Sulfonated Carbon-silica Composites from Sucrose Dispersed on MCM-48. *Chem. Eng. J.* 148(1): 201-206.
- Hasegawa, G., Kanamori, K., Nakanishi, K., Hanada, T. (2010). Fabrication of Activated Carbons with Well-defined Macropores Derived from Sulfonated Poly(divinylbenzene) Networks. *Carbon.* 48(6): 1757-1766.
- Peng, L., Philippaerts, A., Ke, X., Van Noyen, J., De Clippel, F., Van Tendeloo, G., Sels, B. F. (2010). Preparation of Sulfonated Ordered Mesoporous Carbon and its Use for the Esterification of Fatty Acids. *Catal. Today.* 150(1-2): 140-146.
- Poh, N.E., Nur, H., Muhid, M.N.M., Hamdan, H. (2006). Sulphated AIMCM-41: Mesoporous solid Brønsted Acid Catalyst for Dibenzoylation of Biphenyl. *Catal. Today.* 114(2-3): 257-262.

- [14] Selvaraj, M., Pandurangan, A., Seshadri, K.S., Sinha, P.K., Krishnasamy, V., Lal, K.B. (2003). Synthesis of Ethyl β -naphthyl Ether (neroline) using $\text{SO}_4^{2-}/\text{Al-MCM-41}$ mesoporous molecular sieves. *J. Mol. Catal. A: Chem.* 192(1-2): 153-170.
- [15] Nur, H., Manan, A.F.N.A., Wei, L. K., Muhid, M.N.M., Hamdan, H. (2005). Simultaneous Adsorption of a Mixture of Paraquat and Dye by NaY Zeolite Covered with Alkylsilane. *J. Hazard. Mater. B.* 117: 35-40.
- [16] Chao, H.P., Peng, C.L., Lee, C.K., Han, Y.L. (2012). A Study on Sorption of Organic Compounds with Different Water Solubilities on Octadecyltrichlorosilane-modified NaY Zeolite. *J. Taiwan Inst. Chem. Eng.* 43(2):195-200.

JURNAL

ORIGINALITY REPORT

9%

SIMILARITY INDEX

0%

INTERNET SOURCES

0%

PUBLICATIONS

9%

STUDENT PAPERS

PRIMARY SOURCES

1

Submitted to Universiti Teknologi Malaysia

Student Paper

9%

Exclude quotes Off

Exclude matches Off

Exclude bibliography On